IEEE Photonics Journal
An IEEE Photonics Society Publication

Open Access

Group-Delay Control in Two-Port Devices With Dual Input

Volume 5, Number 2, April 2013

P. Acebal
L. Carretero
S. Blaya

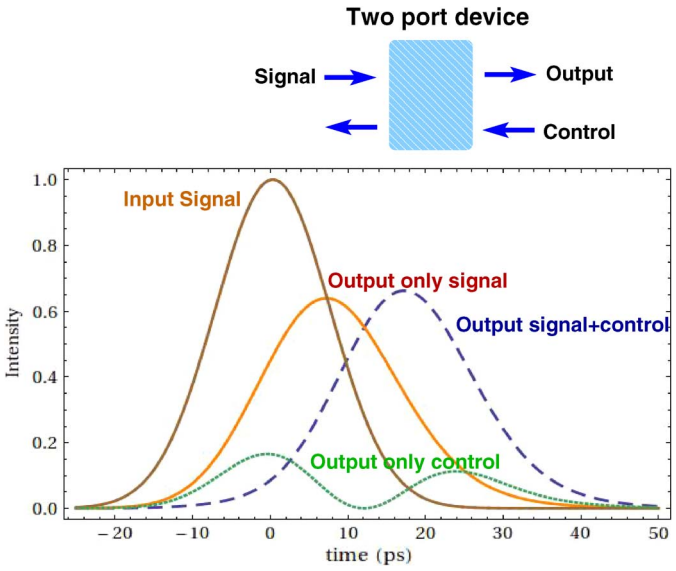

DOI: 10.1109/JPHOT.2013.2251871
1943-0655/$31.00 ©2013 IEEE

Group-Delay Control in Two-Port Devices With Dual Input

P. Acebal, L. Carretero, and S. Blaya

Departamento de Ciencia de Materiales, Óptica y Tecnología Electrónica,
Universidad Miguel Hernández, 03202 Elche, Spain

DOI: 10.1109/JPHOT.2013.2251871
1943-0655/$31.00 ©2013 IEEE

Manuscript received January 10, 2013; revised February 23, 2013; accepted March 2, 2013. Date of publication March 15, 2013; date of current version March 27, 2013. This work was supported in part by Ministerio de Ciencia e Innovación of Spain through Project FIS2009-11065 and in part by the Consellería d'Educació, Formació i Ocupació de la Generalitat Valenciana through Project ACOMP/2012/151. Corresponding author: P. Acebal (e-mail: pablo@dite.umh.es).

Abstract: We present a theoretical and experimental study on the effect of a control field over the temporal propagating characteristics of the signal field in a two-port device. We show that the time delay obtained by the two-port device for the signal field can be greatly modified by the employment of a control field, and therefore, this second input can be used to design devices with tunable group delay. This has been experimentally demonstrated by using a beam splitter plate as two-port system. Furthermore, we analyze the effect of the dual input for a fiber Bragg grating, where it is possible to significantly enhance the time delay with the appropriate control field.

Index Terms: Slow light, scattering matrix.

1. Introduction

In recent years, slow-light phenomena have attracted great interest due to their potential applications [1] such as optical processing, pulse buffering [2], [3], and interferometry [4], [5]. The ability to slow down the group velocity (ν_G) of a propagating pulse implies controlling the frequency dependence of the refractive index by using two different mechanisms: strong material dispersion [6] or structural dispersion [7]. After an initial demonstration of ultraslow group velocities of light pulses by Hau *et al.* [8], several methodologies have been used, which exploit the two mechanisms mentioned above. Hence, for example, material dispersion has been obtained through electromagnetically induced transparency (EIT) resonances [9]–[11], coherent population oscillations [12], [13], or atomic double resonances [14], [15], while structural dispersion has been obtained employing photonic crystal waveguides [16]–[18], coupled resonator optical waveguides (CROWs) [3], [19]–[21], or stimulated Brillouin scattering (SBS) in optical fibers [22], [23].

In principle, one of the major drawbacks of structural dispersion is that these systems are passive in nature, i.e., there is no easy way to change the dielectric constant profile of the medium, so they are not tunable. However, different mechanisms have been studied in order to make these systems tunable. Thus, tunable group delay for structural slow light has been demonstrated using active fiber Bragg gratings (FBGs) [24], [25] or by employing electrooptically tunable microring resonators [26], [27]. Recently, Ang *et al.* [28] showed that it is also possible to obtain a tunable time delay system using a microresonator with dual contrapropagating inputs of the same frequency. In this way, we will demonstrate that such behavior can be obtained by any symmetric two-port device with dual input, where one of the inputs acts as a control field, which changes the temporal propagating characteristics of the signal field. Therefore, depending on the control field used and the

propagating characteristics of the optical element (transmittance and reflectance), this mechanism makes it possible to design devices with tunable time delay or enhance the time delay obtained by structural dispersion. It can be highlighted that, with this methodology, it is possible to obtain delayed signals with relatively high transmittance. In the same way, compared with other all-optical tunable delay systems, as those based on pump–probe mechanism [29], [30], our system exhibit low power consumption, since the intensity of the control beam must be of the same magnitude of the signal beam, while the pump beam (control) usually was significantly greater than the probe beam (signal).

This paper is organized as follows. First, the theoretical background section shows the analytical formulas for the time delay of a two-port system, considering two different contributions, i.e., one due to direct propagation of the signal field through the device and the other one due to the presence of the control field, which initially can take any form, i.e., it will not be equal to the signal field. The results and discussion section provides two examples of how to use the control field in order to modify the time delay. First, we show theoretically and experimentally that the interference mechanism can convert a simple beam splitter plate into a tunable group-delay device. Second, we show that, using the right control field, the time delay obtained by an FBG can be significantly modified.

2. Theoretical Background

The outgoing and incoming fields of a linear optical element are related through the Electromagnetic Scattering Matrix (S-matrix) [31], [32]. In the particular case of a reciprocal two-port device (two inputs and two outputs), such relation can be written as

$$\begin{pmatrix} b_1(\omega) \\ b_2(\omega) \end{pmatrix} = e^{\imath\theta_\tau(\omega)} \begin{pmatrix} \rho(\omega)e^{\imath\left(\theta_\rho(\omega)-\theta_\tau(\omega)\right)} & \tau(\omega) \\ \tau(\omega) & -\rho(\omega)e^{\imath\left(-\theta_\rho(\omega)+\theta_\tau(\omega)\right)} \end{pmatrix} \begin{pmatrix} a_1(\omega) \\ a_2(\omega) \end{pmatrix} \tag{1}$$

where the elements of the S-matrix are expressed as a function of transmittance and reflectance amplitudes of the optical element ($\tau(\omega)$ and $\rho(\omega)$, respectively) and their respective phases [$\theta_\tau(\omega)$ and $\theta_\rho(\omega)$]. It is important to remark that the complex reflectance and transmittance determines the behavior of the optical system in the frequency domain, and their knowledge implies solving the Maxwell equations with appropriate boundary conditions. Now, let us consider two incoming fields, the signal field $a_2(\omega) = \alpha_2(\omega)$, which is a real function of frequency, and the control field $a_1(\omega) = \alpha_1(\omega)\exp[\imath\psi(\omega)]$, which has an amplitude $\alpha_1(\omega)$ and a phase difference of $\psi(\omega)$ with respect to the signal field. Therefore, according to (1), the outgoing field $b_1(\omega)$ is given by

$$b_1(\omega) = \alpha_2(\omega)\tau(\omega)e^{\imath\theta_\tau(\omega)}\left(g(\omega)e^{\imath\chi(\omega)} + 1\right) \tag{2}$$

where we defined the function $g(\omega) = \alpha_1(\omega)\rho(\omega)/\alpha_2(\omega)\tau(\omega)$ as the ratio between the product of control field amplitude and reflectance modulus, and that of transmittance modulus and signal field amplitudes, while $\chi(\omega) = \theta_\rho(\omega) - \theta_\tau(\omega) + \psi(\omega)$ includes the phase functions of reflectance, transmittance, and control signal. As can be seen, in the presence of the control beam, the output field $b_1(\omega)$ not only depends on the input $\alpha_2(\omega)$ and the transmittance of the system but is also a function of the field $a_1(\omega)$ and reflectance of the optical element. Thus, considering that, for a lossless system, the phases of transmittance and reflectance satisfy the condition $\theta_\rho(\omega) - \theta_\tau(\omega) = \pm\pi/2$, for the general case, we consider that this phase difference can be defined as $\theta_\rho(\omega) - \theta_\tau(\omega) = \pm\pi/2 + \vartheta(\omega)$, where the term $\vartheta(\omega)$ takes only nonvanishing values for a system with loss. Therefore, the modulus $\beta_1(\omega)$ and phase $\phi_{b_1}(\omega)$ of the field $b_1(\omega)$ are given by

$$\beta_1(\omega) = \alpha_2(\omega)\tau(\omega)\sqrt{1 + g(\omega)^2 - 2\xi g(\omega)\sin(\Gamma(\omega))} \tag{3}$$

$$\phi_{b_1}(\omega) = \theta_\tau(\omega) + \arctan\left(\frac{\xi g(\omega)\cos(\Gamma(\omega))}{1 - \xi g(\omega)\sin(\Gamma(\omega))}\right) \tag{4}$$

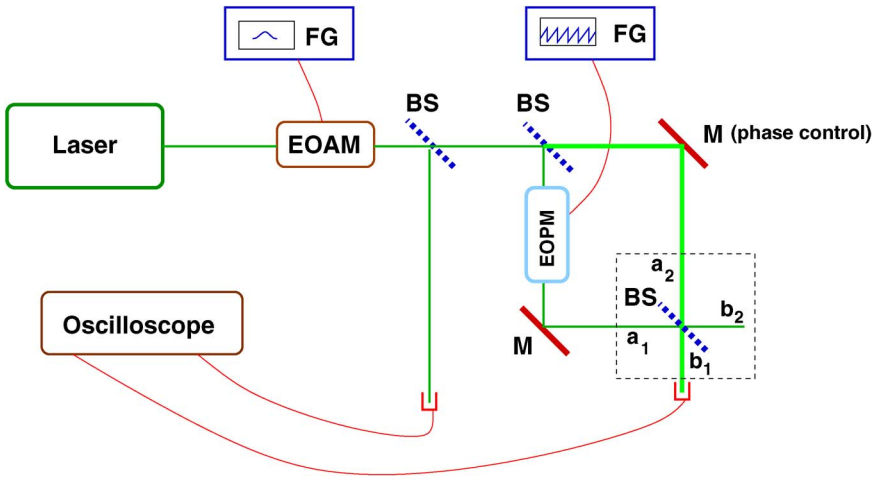

Fig. 1. Scheme of the optical setup employed for measurement of the time delay (BS: beam splitter, M: mirror, FG: function generator).

where ξ is a parameter that takes the value 1 or -1 depending on whether the difference $\theta_\rho(\omega) - \theta_\tau(\omega)$ starts on $\pi/2$ or $-\pi/2$, while $\Gamma(\omega) = \psi(\omega) + \vartheta(\omega)$ takes into account the effect of the phase of the control input together with the effect of the losses in the phase of the reflectance. An interesting result is obtained for the phase of the outgoing signal field $\phi_{b_1}(\omega)$ since, due to the presence of the control signal, new terms appear, which depend on the amplitudes of both signals, i.e., reflectance and transmittance, together with the $\Gamma(\omega)$ function. Therefore, the time delay δ_{b_1} of the signal field after passing through the optical element can be estimated differentiating the phase $\phi_{b_1}(\omega)$ with respect the frequency ω, and we will distinguish two different contributions $\delta_{b_1} = \delta_\tau + \delta_c$, one due to the phase of the transmittance (δ_τ) and the other due to the presence of control field (δ_c), which can be written as

$$\delta_\tau = \theta'_\tau(\omega) \tag{5}$$

$$\delta_c = \frac{\xi g'(\omega)\cos(\Gamma(\omega)) + \left(g^2(\omega) - \xi g(\omega)\sin(\Gamma(\omega))\right)\Gamma'(\omega)}{1 + g(\omega)^2 - 2\xi g(\omega)\sin(\Gamma(\omega))} \tag{6}$$

where δ_τ is the time delay associated with the physical characteristics of the two-port device, like thickness, refractive index dispersion, or structure. However, as can be seen from (6), the delay due to the control field depends on the dispersion of the functions $g(\omega)$ and $\Gamma(\omega)$, which are related to the amplitudes and phases of the control field, the transmittance, and the reflectance. Therefore, this second term can be used to increase the time delay of the optical element or to design an optical system with tunable delay using the appropriate control field. As examples, we will study two cases in order to demonstrate two different ways to modify the temporal delay of an optical system with the control field.

3. Results and Discussion

3.1. Beam Splitter Plate

Let us start the study of the effect of the control beam theoretically and experimentally for a simple system by analyzing the time delay produced by a beam splitter plate with dual input formed by very narrow pulses in the frequency domain (i.e., high bandwidth in the time domain). A scheme of the optical setup employed for the experimental measurement is shown in Fig. 1. The continuous beam generated by a Nd:VO_4 laser passes through an electrooptic amplitude modulator (EOAM), which generates a Gaussian pulse of the desired temporal width (σ). The beam then crosses two beam splitters, where the first was used to create a reference signal, while the second one

produces the signal and control fields. Finally, two mirrors redirect the signal and control fields to the last beam splitter, which acts as the two-port system giving the tunable time delay. The mirror on the signal field arm was controlled with a micropositioning system in order to select the phase difference between the two fields, while the control field arm includes an electrooptic phase modulator (EOPM), which was used to modify the functional dependence of the control beam on the frequency. Specifically, we used the EOPM in order to modify the carrier frequency of the control field. This was done using a periodic positive ramp temporal function with the amplitude required to change the phase of the control beam between 0 and 2π, so the displacement of the carrier frequency was given by the frequency of the temporal function used. It is important to note that, although the experimental setup seems to be a Mach–Zehnder interferometer, we are not analyzing the time delay generated by such interferometer, since the control and signal fields can be generated with other experimental setup, but this is an easy way to generate both fields in the laboratory.

In this case, we assume that the two-port system is not dispersive, i.e., there is no frequency dependence for τ, ρ, and θ_τ over the region of interest ($\tau = \rho = \sqrt{2}/2$ and θ_τ is constant for all the frequencies of the pulse), and without loss $[\Gamma(\omega) = \psi(\omega)]$. So according to (4) and (5), there is no delay of the signal field in the absence of a control field (the time delay produced by the transmittance is negligible compared with the width of the pulse). Furthermore, a constant phase difference between control and signal fields $(\psi(\omega) = \psi_0)$ was used, i.e., no significant difference between the optical path length of control and signal beams, so the only source of time delay for this system is the derivative with respect to the frequency of $g(\omega)$, which now only depends on the control and signal field amplitudes $(g(\omega) = \alpha_1(\omega)/\alpha_2(\omega))$. Therefore, it is important to note that, in order to obtain a time delay, the two amplitudes must not have the same frequency dependence. This was achieved by simply changing the carrier frequency of the control field, so the amplitudes are easily obtained after the corresponding Fourier transform of the respective time-dependent input fields [the same Gaussian envelope with different carrier frequencies ω_υ, $a_\upsilon(t) = \exp(-t^2/2\sigma^2)\exp(\imath\omega_\upsilon t)$] and are given by

$$\alpha_2(\omega) = e^{-(\omega-\omega_0)^2\sigma^2/2} \tag{7}$$

$$\alpha_1(\omega) = e^{-(\omega-\omega_0-\Delta\omega_0)^2\sigma^2/2} \tag{8}$$

where σ denotes the temporal width of the Gaussian pulse, and $\Delta\omega_0$ is the displacement of the carrier frequency of the control field produced by the EOPM. Introducing amplitudes (7) and (8) into (6), the delay obtained for the b_1 output can be written as

$$\delta_{b_1} = \frac{\Delta\omega_0\sigma\cos(\psi_0)}{2(\cosh((2\omega' - \Delta\omega_0)\Delta\omega_0\sigma^2/2) - \sin(\psi_0))} \tag{9}$$

where $\omega' = \omega - \omega_0$ defines the displacement of the frequency with respect to the carrier of the signal beam. Equation (9) takes a form similar to a Lorentzian function centered on the average value of the two carrier frequencies, where its magnitude depends on three parameters $\Delta\omega_0$, σ, and the phase difference ψ_0. This last parameter is not only responsible for the value of the time delay but also determines the sign, so it is possible to obtain fast or slow light by selecting the appropriate value of ψ_0. Specifically, for this optical system, superluminal group velocity can be obtained for values of ψ_0 in the interval $[-\pi/2 : \pi/2]$, while subluminal light can be obtained for values between $\pi/2$ and $3\pi/2$. This can be seen in the simulations shown on the left-hand side of Fig. 2, where we plotted the time delay in the presence of a control field for different values of the parameters. As mentioned above, the behavior of the time delay corresponds to a Lorentzian function, which is positive for ψ_0 values less than $\pi/2$, while negative time delay is obtained for ψ_0 values higher than $\pi/2$. The magnitude of the time delay increases as the phase difference ψ_0 approaches to $\pi/2$, so for example, a maximum time delay of 0.073 s is obtained for $\psi_0 = \pi/2 - 1.7$, whereas a value of 0.27 s can be reached with a phase difference of $\psi_0 = \pi/2 - 0.6$.

However, the increase in time delay also implies greater deformation of the modulus of the output field b_1 in the frequency domain as shown on the right-hand side of Fig. 2, and thus, there will be a

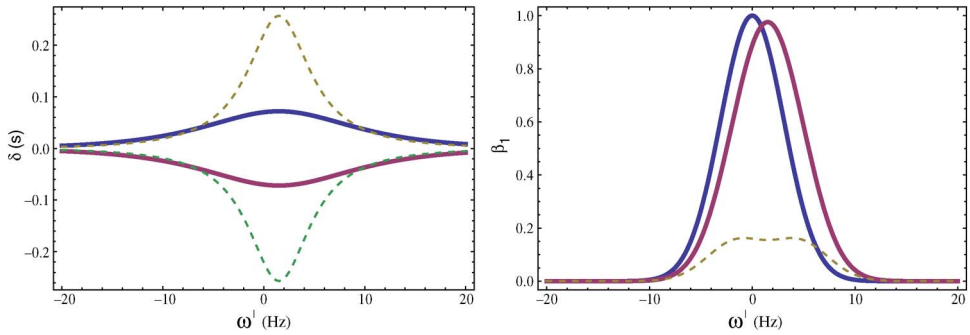

Fig. 2. (Left) Simulation of the time delay δ_{b_1} dependence with ω' in the presence of a control field with the parameter values $\sigma = 0.23$ s, $\Delta\omega_0 = \pi$ Hz and different values of ψ_0 ($\psi_0 = \pi/2 + 1.7$: magenta, $\psi_0 = \pi/2 - 1.7$: blue, $\psi_0 = \pi/2 + 0.6$: green, $\psi_0 = \pi/2 - 0.6$: yellow). (Right) Simulation of the intensity profile of the b_1 field for three different cases: reference signal (blue), control field with a phase difference of $\psi_0 = \pi/2 \pm 1.7$ (magenta) and control field with a phase difference of $\psi_0 = \pi/2 \pm 0.6$ (yellow). The values of the other parameters used in simulation were $\sigma = 0.23$ s and $\Delta\omega_0 = \pi$ Hz.

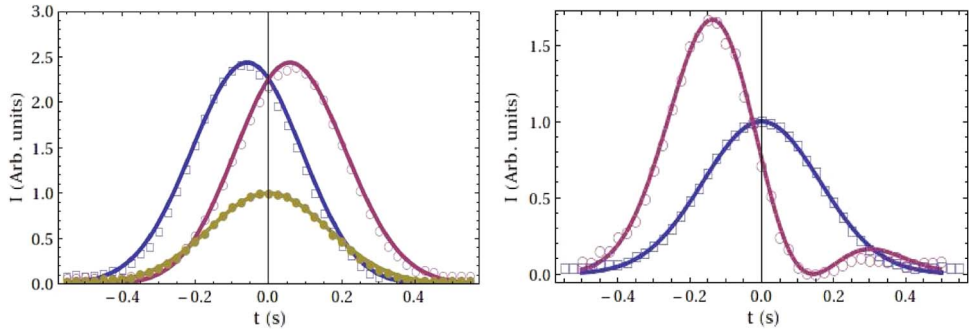

Fig. 3. (Left) Experimental (points) and theoretical (continuous line) intensity distributions of the reference signal (brown) and output signal b_1 ($\psi_0 = \pi/2 + 1.7$: blue, $\psi_0 = \pi/2 - 1.7$: magenta) in the presence of control field (the values employed for the other parameters were $\sigma = 0.23$ s, $\Delta\omega_0 = \pi$ Hz) (Right) Experimental (points) and theoretical (continuous line) intensity distributions of the reference signal (blue) and output signal b_1 (magenta) in the presence of the control field (we used the following parameter values: $\sigma = 0.23$ s, $\Delta\omega_0 = 2\pi$ Hz and $\psi_0 = \pi/2 + 0.9$).

great deformation of the pulse in the time domain. As can be seen, the intensity profile for $\psi_0 = \pi/2 \pm 1.7$ retains the Gaussian distribution of the input signal but, in this case, centered on the frequency $\omega' = \Delta\omega_0/2$, as in the case of time delay but a little wider, while for $\psi_0 = \pi/2 \pm 0.6$, greater deformation of the Gaussian distribution is observed. In the same way, larger values of time delay also imply smaller values of the maximum intensity of the signal b_1, i.e., the *losses* also increase, where the term *losses* refers to the intensity of the output b_2.

Finally, we can analyze the effect in the time domain by simply doing the inverse Fourier transform of the output signal $b_1(\omega)$, so the intensity of the output pulse is $I(t) = |\mathrm{FT}^{-1}[b_1(\omega)]|^2$. Fig. 3 shows theoretical and experimental intensity distributions in the time domain for the optical setup employed here. As can be seen, both superluminal and subluminal group velocity can be observed by tuning the phase difference ψ_0. The left-hand side of the Fig. 3 shows that the pulse may be advanced or delayed the same amount by adding or subtracting a given value to $\pi/2$ of the phase difference. As can be seen, a very good agreement between theoretical predictions and experimental measurements was found. In the case of $\psi_0 = \pi/2 \pm 1.7$, the temporal delay (or advance) of the output pulse obtained was around 0.06. The right-hand side of Fig. 3 shows the theoretical and experimental pulse delay data for different working conditions, which, in principle, increase the time delay, since we increase the displacement of the carrier frequency and use a phase difference closer to $\pi/2$ than that used in the case shown on the left. As can be seen, with

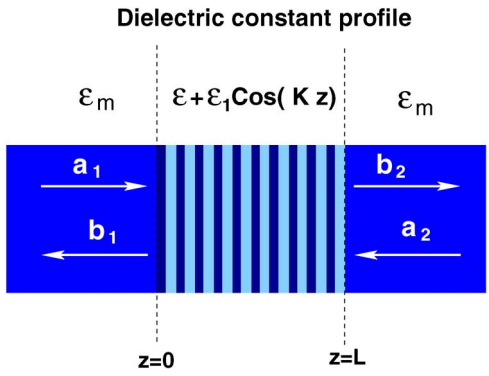

Fig. 4. Scheme of the configuration studied for a Reflection Bragg grating.

these conditions, the output signal advanced 0.15 s with respect to the reference signal but with a greater deformation of the pulse envelope, since, in this case, a secondary lobe appears delayed by about 0.3 s with respect to the reference signal. We also want to note that the output signal has more intensity than that of the input signal due to the contribution of the control beam. So for example, for the control beam with $\Delta\omega_0 = \pi$ Hz, the output signal has a maximum intensity 2.5 times that of the input signal, which is a probe of the interferential nature of the group delay for these systems.

3.2. Reflection Bragg Grating

The second case that we are going to analyze is a reflection Bragg grating with dual input. The reflection Bragg grating is a typical example of a system that exhibits slow light due to the material structure and has been studied extensively, usually in the field of fiber optics applications [24], [33], [34]. However, the studies in the bibliography usually use the approximation given by the coupled wave theory (CWT) to study the effect of material structure on the group velocity [33], [34], while in our case, we use the exact solution of the Helmholtz equation for the Bragg grating [35]. The main reason for doing this is that the solution given by the CWT does not fulfill the condition $\theta_\rho(\omega) - \theta_\tau(\omega) = \pm\pi/2$ for a FBG without loss (i.e., $\vartheta(\omega)$ is not zero for CWT), which was a requirement for all the systems without loss, as mentioned in the theoretical background. Therefore, we use the exact transmittance and reflectance coefficients for a dielectric constant like that shown in Fig. 4. Details of the procedure to obtain such coefficients can be found in reference [35], which can be expressed in reduced form as

$$t = \frac{\eta_1^u \mu_{-1}^u - \eta_{-1}^u \mu_1^u}{\eta_{-1}^v \mu_1^u - \eta_1^u \mu_{-1}^v} = \tau_B(\omega) e^{\imath\theta_{\tau_B}(\omega)} \tag{10}$$

$$r = \frac{\eta_1^v \mu_1^u - \eta_1^u \mu_1^v}{\eta_{-1}^v \mu_1^u - \eta_1^u \mu_{-1}^v} = \rho_B(\omega) e^{\imath\theta_{\rho_B}(\omega)} \tag{11}$$

where the functions η_κ^q and μ_κ^q are combinations of the Mathieu cosine $C(q)$ and Mathieu sine $S(q)$ functions and their derivatives, which can be written as

$$\eta_\kappa^q = \zeta_1 C(q) + \imath\kappa\zeta_2 C'(q) \tag{12}$$

$$\mu_\kappa^q = \zeta_1 S(q) + \imath\kappa\zeta_2 S'(q) \tag{13}$$

where the characteristic parameters q are given by two different sets, called u and v, which are given by

$$u = \left(\zeta_1^2, -\zeta_3\zeta_1^2, \zeta_4\right) \qquad v = \left(\zeta_1^2, -\zeta_3\zeta_1^2, 0\right). \tag{14}$$

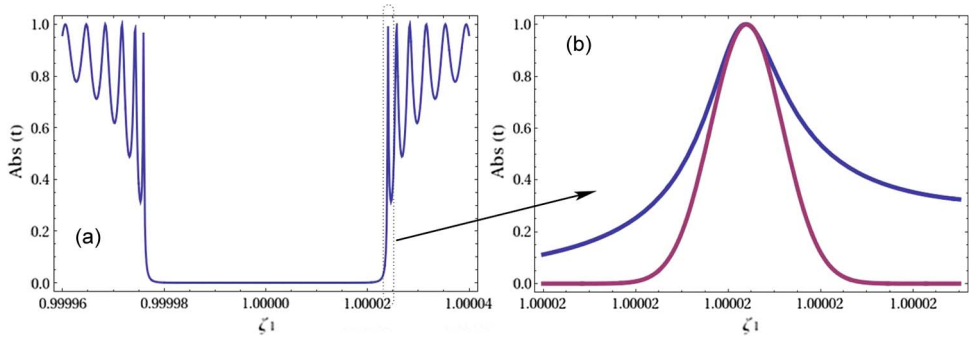

Fig. 5. (a) Transmittance spectrum of a FBG with parameters: $\epsilon = \epsilon_m = 2.1083$, $\epsilon_1 = 2 \times 10^{-4}$, $\omega_g = 1.22894 \times 10^{15}$ s^{-1} and $L = 0.1$ meters. (b) Transmittance spectrum (blue color) and normalized pulse intensity (magenta color) around the first transmittance maximum for the same FBG parameters than (a).

Finally, the ζ_i coefficients are defined as

$$\zeta_1 = \frac{\omega}{\omega_g} \quad \zeta_2 = \sqrt{\frac{\epsilon}{\epsilon_m}} \quad \zeta_3 = \frac{\epsilon_1}{2\epsilon} \quad \zeta_4 = L\sqrt{\epsilon}\omega_g/c \tag{15}$$

where ω_g is the central frequency for which the grating is designed, ϵ_m is the dielectric constant of the surrounding medium, ϵ is the average dielectric constant of the grating, while ϵ_1 is the dielectric constant modulation, and L is the grating length. As a function of all of these parameters, it is possible to obtain the time delay from femtoseconds to picoseconds, but in all the cases, the Bragg grating acts as a passive device for optical pulse manipulation.

In our case, we are going to show how the presence of the control field converts this passive element into an active device with tunable time delay. In order to do this, let us analyze the case of a FBG with standard values for the design parameters ($\epsilon = \epsilon_m = 2.1083$, $\epsilon_1 = 2 \times 10^{-4}$, $\omega_g = 1.22894 \times 10^{15}$ s^{-1}, and $L = 0.1$ meters), whose transmittance spectrum as a function of the ζ_1 variable is shown in the upper part of Fig. 5 for two different scales. Fig. 5(a) shows the spectrum over a wide range of values of ζ_1, which is characterized by a wide central reflection band with high efficiency and multiple narrower lobes with lower efficiencies. Since the main requirement of any device is the minimization of losses, we selected a signal field with a Gaussian envelope $(a(t) = \exp(-t^2/2\sigma^2)\exp(-i\omega_0 t))$ whose carrier frequency $(\omega_0 = \omega_g + \Delta\omega_0)$ was centered on the first maximum of transmittance $(\Delta\omega_0 = 29.5$ Ghz$)$ and whose width in the frequency domain was set obtain distortionless transmission $(\sigma = 7.4$ ps$)$. Fig. 5(b) shows in detail the transmittance spectrum around the first maximum and the normalized signal field in the frequency domain. Without the presence of a control field, the Bragg grating acts as a passive device for the input pulse, for which the time delay can be estimated by differentiating the phase of the transmittance with respect to ω. In the case of the values used for the FBG, the time delay of the transmittance is shown in Fig. 6(a). As can be seen, the FBG time delay is similar to a Lorentzian curve centered at the frequency of maximum transmittance (which is the same as the carrier frequency of the selected pulse), whose maximum value is about 10 ps. The temporal response of the transmitted pulse, together with the reference pulse (pulse that travels a distance L in a medium with dielectric constant ϵ), can be seen in Fig. 6(b) and (c). Basically, the pulse undergoes a delay of about 7 ps due to the effect of the Bragg grating, which implies an approximate ratio of 1 between the time delay and the pulsewidth. Also, a slight temporal broadening was observed due to the frequency filtering, since, as can be seen in Fig. 5(b), the transmittance amplitude is different for all the frequencies of the pulse.

The time delay obtained by the Bragg grating can be substantially modified by the presence of a control field, since, as explained in the theoretical background, this field adds an extra contribution to the time delay of the output signal, which depends on the amplitude of the control beam in the

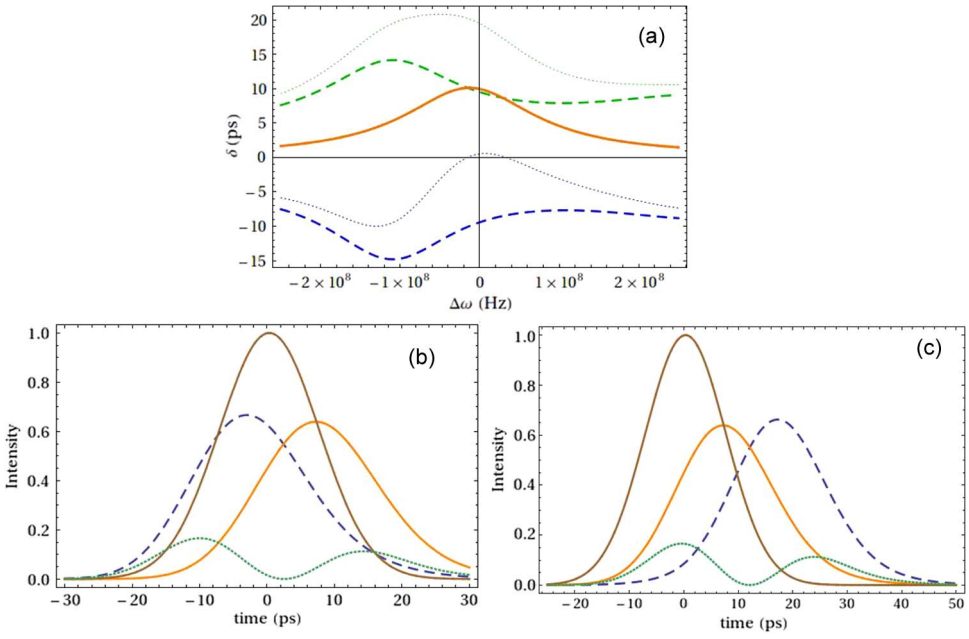

Fig. 6. (a) Time delay of the transmittance of FBG δ_τ (continuous line), and contributions due to the interference with control fields (δ_c) with phase difference $\psi_1(\omega) = -\sigma(\omega - \omega_0) - \pi/4$ (blue dashed line) and $\psi_2(\omega) = \sigma(\omega - \omega_0) + 5\pi/8$ (green dashed line) versus the frequency detuning $(\Delta\omega)$ with respect to the carrier frequency $(\omega = \omega_0 + \Delta\omega)$. The dotted line represents the total time delay δ_{b_i} as the sum of the two contributions for the two different control fields, respectively. (b) Intensity of the signal beam without grating (brown continuous line), signal beam without control beam (orange continuous line), control beam without signal beam $[\psi(\omega) = -\sigma(\omega - \omega_0) - \pi/4$ (green short dashed line)], and signal beam with control field $[\psi(\omega) = -\sigma(\omega - \omega_0) - \pi/4$ (blue long dashed line)]. (c) Intensity of the signal beam without grating (brown continuous line), signal beam without control beam (orange continuous line), control beam without signal beam $[\psi(\omega) = \sigma(\omega - \omega_0) + \pi/8$ (green short dashed line)], and signal beam with control field $[\psi(\omega) = \sigma(\omega - \omega_0) + \pi/8$ (blue long dashed line)].

frequency domain, the relative phase difference between both fields, and the reflectance and transmittance of the device. For example, let us consider a control field, which is identical to the signal field $(\alpha_1(\omega) = \alpha_2(\omega))$, but that impinges on the device with a linear phase difference with respect to ω, which can be written as

$$\psi(\omega) = \gamma(\omega - \omega_0) + \psi_0 \tag{16}$$

where γ is a parameter with dimensions of time, which basically determines the delay with which the control field impinges on the device with respect to the signal field, while ψ_0 denotes the difference of phase origin between both fields. In this case, the $g(\omega)$ function only depends on the transmittance and reflectance amplitudes $(g(\omega) = \rho_B(\omega)/\tau_B(\omega) = \sqrt{1 - \tau_B(\omega)^2}/\tau_B(\omega))$. Therefore, the new contribution to the time delay due to the control beam can be written as

$$\delta_c = \frac{\xi\tau_B'(\omega)\cos(\psi(\omega)) + \gamma\rho_B(\omega)^2(\xi\sin(\psi(\omega))\tau_B(\omega) - \rho_B(\omega))}{\rho_B(\omega)(2\xi\tau_B(\omega)\rho_B(\omega)\sin(\psi(\omega)) - 1)} \tag{17}$$

where $\tau'(\omega)$ denotes the derivative of the transmittance amplitude with respect to the frequency. Now, let us analyze the effect of two different control fields, one with a phase difference $\psi_1(\omega) = -\sigma(\omega - \omega_0) - \pi/4$ and the other one with a phase difference $\psi_2(\omega) = \sigma(\omega - \omega_0) + 5\pi/8$. Fig. 6(a), shows the δ_c contribution for these two different $\psi(\omega)$ values, which is also compared with the contribution of the transmittance δ_τ. As can be seen, the maximum (or minimum, depending on the sign) of the time delay due to the control beam δ_c shifted with respect to the carrier frequency, and the time delay exhibited a smoother behavior than δ_τ, so nonvanishing values were obtained over all the frequency detuning range plotted (2.5 times the pulsewidth in the frequency domain). It is

important to note that, as in the case of the beam splitter plate, the phase difference $\psi(\omega)$ determines the sign of the contribution δ_c, so for $\psi_1(\omega)$ and $\psi_2(\omega)$, the time delay δ_c has the same behavior but with the opposite sign. Thus, in the presence of a control field with $\psi_2(\omega)$, the total time delay of the output signal is approximately twice that obtained by the Bragg grating for the carrier frequency and greater for the other frequencies, while for a control field with $\psi_1(\omega)$, δ_c cancels out δ_τ for the carrier frequency and has negative time delay for the other frequencies.

Finally, the simulations of the output pulse in the time domain for all these configurations are shown in Fig. 6(b) and (c). As can be seen, the output pulse for the control beam with $\psi_2(\omega)$ is delayed for 18 ps with respect to the reference pulse, so the ratio between delay and pulsewidth becomes approximately 2.4, which is double that obtained only with the Bragg grating. Also, it should be noted that this delay is obtained with low loss with respect to the original pulse, since the output intensity is about 0.7 times of the input pulse intensity. An interesting result is also obtained by the control beam with $\psi_1(\omega)$, for which superluminal behavior is observed, so the output pulse advanced for 3.5 ps with respect to the reference one. Therefore, we showed that the interference with a control beam can be used to tune the time delay of a FBG, changing the behavior from subluminal to superluminal.

4. Conclusion

In conclusion, we have demonstrated that a two-port systems with dual input can be used to design a tunable time delay systems or to significantly enhance the time delay obtained by only one input. In this way, we have deduced the analytical formulas for the effect of the control field on the propagating characteristics of the signal field. This has been analyzed for two different systems, a beam splitter plate and a FBG. In the first case, we have shown that slow or fast light can be obtained as a function of the phase difference between the two inputs, where the control field is slightly different from the signal field. In the second case, we have demonstrated that, with the appropriate control field, the interference mechanism enhanced the time delay obtained by the FBG by a factor of three and that fast light can also be obtained.

Acknowledgment

The authors wish to thank the anonymous reviewers for their valuable suggestions.

References

[1] R. Boyd, O. Hess, C. Denz, and E. Paspalkalis, "Slow light," *J. Opt.*, vol. 12, no. 10, p. 100301, Oct. 2010.
[2] J. B. Khurgin, "Optical buffers based on slow light in electromagnetically induced transparent media and coupled resonator structures: Comparative analysis," *J. Opt. Soc. Amer. B*, vol. 22, no. 5, pp. 1062–1074, May 2005.
[3] F. N. Xia, L. Sekaric, and Y. Vlasov, "Ultracompact optical buffers on a silicon chip," *Nat. Photon.*, vol. 1, no. 1, pp. 65–71, Jan. 2007.
[4] Z. Shi, R. W. Boyd, R. M. Camacho, P. K. Vudyasetu, and J. C. Howell, "Slow-light Fourier transform interferometer," *Phys. Rev. Lett.*, vol. 99, no. 24, pp. 240801-1–240801-4, Dec. 2007.
[5] Z. M. Shi, R. W. Boyd, D. J. Gauthier, and C. C. Dudley, "Enhancing the spectral sensitivity of interferometers using slow-light media," *Opt. Lett.*, vol. 32, no. 8, pp. 915–917, Apr. 2007.
[6] R. Boyd and D. J. Gauthier, "'Slow' and 'fast' light," in *Progress in Optics*, E. Wolf, Ed. Amsterdam, The Netherlands: Elsevier, 2002, pp. 497–530.
[7] R. W. Boyd, "Material slow light and structural slow light: Similarities and differences for nonlinear optics," *J. Opt. Soc. Amer. B.*, vol. 28, no. 12, pp. A38–A44, Dec. 2011. [Online]. Available: http://josab.osa.org/abstract.cfm?URI=josab-28-12-A38
[8] L. V. Hau, S. E. Harris, Z. Dutton, and C. H. Behroozi, "Light speed reduction to 17 metres per second in an ultracold atomic gas," *Nature*, vol. 397, no. 6720, pp. 594–598, Feb. 1999.
[9] A. Kasapi, M. Jain, G. Y. Yin, and S. E. Harris, "Electromagnetically induced transparency—Propagation dynamics," *Phys. Rev. Lett.*, vol. 74, no. 13, pp. 2447–2450, Mar. 1995.
[10] M. D. Lukin, "Colloquium: Trapping and manipulating photon states in atomic ensembles," *Rev. Mod. Phys.*, vol. 75, no. 2, pp. 457–472, Apr. 2003.
[11] L. V. Hau, "Optical information processing in Bose–Einstein condensates," *Nat. Photon.*, vol. 2, no. 8, pp. 451–453, Aug. 2008.
[12] M. S. Bigelow, N. N. Lepeshkin, and R. W. Boyd, "Superluminal and slow light propagation in a room-temperature solid," *Science*, vol. 301, no. 5630, pp. 200–202, Jul. 2003.

[13] M. S. Bigelow, N. N. Lepeshkin, and R. W. Boyd, "Observation of ultraslow light propagation in a ruby crystal at room temperature," *Phys. Rev. Lett.*, vol. 90, no. 11, p. 113903, Mar. 2003.
[14] R. M. Camacho, M. V. Pack, and J. C. Howell, "Low-distortion slow light using two absorption resonances," *Phys. Rev. A*, vol. 73, no. 6, pp. 063812-1–063812-4, Jun. 2006.
[15] R. M. Camacho, C. J. Broadbent, I. Ali-Khan, and J. C. Howell, "All-optical delay of images using slow light," *Phys. Rev. Lett.*, vol. 98, no. 4, p. 043902, Jan. 2007.
[16] Y. A. Vlasov, M. O'Boyle, H. F. Hamann, and S. J. McNab, "Active control of slow light on a chip with photonic crystal waveguides," *Nature*, vol. 438, no. 7064, pp. 65–69, Nov. 2005.
[17] T. Baba, "Slow light in photonic crystals," *Nat. Photon.*, vol. 2, no. 8, pp. 465–473, Aug. 2008.
[18] M. Notomi, "Manipulating light with strongly modulated photonic crystals," *Rep. Progr. Phys.*, vol. 73, no. 9, p. 096501, Sep. 2010.
[19] A. Yariv, Y. Xu, R. K. Lee, and A. Scherer, "Coupled-resonator optical waveguide: A proposal and analysis," *Opt. Lett.*, vol. 24, no. 11, pp. 711–713, Jun. 1999.
[20] D. D. Smith, H. Chang, K. A. Fuller, A. T. Rosenberger, and R. W. Boyd, "Coupled-resonator-induced transparency," *Phys. Rev. A*, vol. 69, no. 6, p. 063804, Jun. 2004.
[21] L. Carretero, S. Blaya, P. Acebal, A. Fimia, R. Madrigal, and A. Murciano, "Coupled wave analysis of holographically induced transparency (HIT) generated by two multiplexed volume gratings," *Opt Exp.*, vol. 19, no. 8, pp. 7094–7105, Apr. 2011.
[22] Z. M. Zhu, A. M. C. Dawes, D. J. Gauthier, L. Zhang, and A. E. Willner, "Broadband SBS slow light in an optical fiber," *J. Lightwave Technol.*, vol. 25, no. 1, pp. 201–206, Jan. 2007.
[23] L. Thevenaz, "Slow and fast light in optical fibres," *Nat. Photon.*, vol. 2, no. 8, pp. 474–481, Aug. 2008.
[24] S. Longhi, "Group delay tuning in active fiber Bragg gratings: From superluminal to subluminal pulse reflection," *Phys. Rev. E*, vol. 72, no. 5, p. 056614, Nov. 2005.
[25] K. Qian, L. Zhan, H. Li, X. Hu, J. Peng, L. Zhang, and Y. Xia, "Tunable delay slow-light in an active fiber Bragg grating," *Opt. Exp.*, vol. 17, no. 24, pp. 22 217–22 222, Nov. 2009. [Online]. Available: http://www.opticsexpress.org/abstract.cfm?URI=oe-17-24-22217
[26] A. Guarino, G. Poberaj, D. Rezzonico, R. Degl'Innocenti, and P. Günter, "Electro-optically tunable microring resonators in lithium niobate," *Nat. Photon.*, vol. 1, no. 7, pp. 407–410, Jul. 2007.
[27] T.-J. Wang, C.-H. Chu, and C.-Y. Lin, "Electro-optically tunable microring resonators on lithium niobate," *Opt. Lett.*, vol. 32, no. 19, pp. 2777–2779, Oct. 2007. [Online]. Available: http://ol.osa.org/abstract.cfm?URI=ol-32-19-2777
[28] T. Y. L. Ang and N. Q. Ngo, "Tunable fast and slow light in a traveling wave microresonator via interaction of intra-cavity backscattering with dual contrapropagating inputs," *J. Opt. Soc. Amer. B.*, vol. 27, no. 12, pp. 2774–2783, Dec 2010. [Online]. Available: http://josab.osa.org/abstract.cfm?URI=josab-27-12-2774
[29] P. Acebal, S. Blaya, L. Carretero, R. F. Madrigal, and A. Fimia, "Rigorous analysis of the propagation of sinusoidal pulses in bacteriorhodopsin films," *Opt. Exp.*, vol. 20, no. 23, pp. 25 497–25 512, Nov. 2012.
[30] C. S. Yelleswarapu, R. Philip, F. J. Aranda, B. R. Kimball, and D. V. G. L. N. Rao, "Slow light in bacteriorhodopsin solution using coherent population oscillations," *Opt. Lett.*, vol. 32, no. 13, pp. 1788–1790, Jul. 2007.
[31] H. A. Haus, *Waves and Fields in Optoelectronics*, N. Holonyak, Ed. Englewood Cliffs, NJ, USA: Prentice-Hall, 1984.
[32] L. Li, "Formulation and comparison of two recursive matrix algorithms for modeling layered diffraction gratings," *J. Opt. Soc. Amer. A*, vol. 13, no. 5, pp. 1024–1035, May 1996.
[33] T. Erdogan, "Fiber grating spectra," *J. Lightwave Technol.*, vol. 15, no. 8, pp. 1277–1294, Aug. 1997.
[34] S. Longhi, M. Marano, P. Laporta, O. Svelto, and M. Belmonte, "Propagation, manipulation, and control of picosecond optical pulses at 1.5 μm in fiber Bragg gratings," *J. Opt. Soc. Amer. B*, vol. 19, no. 11, pp. 2742–2757, Nov. 2002.
[35] L. Carretero, M. Perez-Molina, S. Blaya, R. F. Madrigal, P. Acebal, and A. Fimia, "Application of the fixed point theorem for the solution of the 1d wave equation: Comparison with exact Mathieu solutions," *Opt. Exp.*, vol. 13, no. 22, pp. 9078–9084, Oct. 2005.